A FUSION OF A DISCRETE WAVELET TRANSFORM-BASED AND TIME-DOMAIN FEATURE EXTRACTION FOR MOTOR IMAGERY CLASSIFICATION

Fouziah Md Yassin[1], Norita Md Norwawi[2], Nor Azila Noh[3], Afishah Alias[4] and Sofina Tamam[5]

(Received: 20-Nov.-2023, Revised: 1-Feb.-2024, Accepted: 16-Feb.-2024)

ABSTRACT

A motor imagery (MI)-based brain-computer interface (BCI) has performed successfully as a control mechanism with multiple electroencephalogram (EEG) channels. For practicality, fewer EEG channels are preferable. This paper investigates a single-channel EEG signal for MI. However, there are insufficient features that can be extracted due to a single-channel EEG signal being used in one region of the brain. An effective feature extraction technique plays a critical role in overcoming this limitation. Therefore, this study proposes a fusion of discrete wavelet transform (DWT)-based and time-domain feature extraction to provide more relevant information for classification. The highest accuracy obtained on the BCI Competition III (IVa) dataset is 87.5% with logistic regression (LR) while the OpenBMI dataset attained the highest accuracy of 93% with support vector machine (SVM) as the classifier. Addressing the potential of enhancing the performance of a single EEG channel located on the forehead, the achieved result is relatively promising.

KEYWORDS

Motor imagery, Feature extraction, Electroencephalogram (EEG), Discrete wavelet transform, Brain-computer interface.

1. INTRODUCTION

There are two techniques for measuring brain activity: invasive measurement and non-invasive measurement. The non-invasive design was ranked as a high-priority design. It is risk-free and does not require surgery as an invasive necessity, even though the invasive technique is more accurate [1]. An electroencephalogram (EEG) is widely used for non-invasive measurement that records the brain's electrical fields through metal electrodes placed on the scalp with the standard international 10–20 electrode site placement [2]. Besides that, it is relatively inexpensive, has a good temporal resolution, enabling it to accurately capture fluctuations in brain activity throughout time and requires little setup [3]. Additionally, it is highly portable, making it suitable for usage in diverse locations, such as hospital environments, research laboratories and even mobile applications. The EEG is a useful diagnostic tool that is particularly effective in identifying and monitoring neurological illnesses, like Alzheimer's and epilepsy, involving analysis of the EEG recordings to detect abnormal brain activity linked with seizures [4][5][6]. Besides that, it is being used in various non-clinical settings, such as education, emotion detection and control mechanisms, to explore new potentials and applications [7]-[8]. The EEG is utilized in education to investigate and improve cognitive processes, providing valuable information about attention, focus and learning patterns. Furthermore, the EEG plays a crucial role in the advancement of brain-computer interfaces (BCIs) which function as control mechanisms.

BCI links the human brain's electrical activity to an external device, such as a wheelchair or computer system. Neuronal electrical signals in the human brain are detected, interpreted and converted into machine language that corresponds to the user's desires [1]. This technology has significant potential to offer alternative communication channels for those with physical limitations. In BCI, users' comfort is

1. F. M. Yassin is with Faculty of Sci. and Tech., Uni. Sains Islam Malaysia and with Faculty of Science and Natural Resources, Universiti Malaysia Sabah, Sabah, Malaysia. Emails: fouziahy@raudah.usim.edu.my and fouziahy@ums.edu.my
2. N. M. Norwawi is with Cyber Security and System Research Unit, Faculty of Science and Technology, Universiti Sains Islam Malaysia, Negeri Sembilan, Malaysia. Email: norita@usim.edu.my
3. N. Noh is with the Brain and Behaviour Research Group, and Faculty of Medicine and Health Sciences, Universiti Sains Islam Malaysia, Negeri Sembilan, Malaysia. Email: azila@usim.edu.my
4. A. Alias is with the Faculty of Applied Sciences and Technology, Universiti Tun Hussein Onn, Johor, Malaysia. Email: afishah@uthm.edu.my
5. S. Tamam is with the Brain and Behaviour Research Group and Faculty of Science and Technology, Universiti Sains Islam Malaysia, Negeri Sembilan, Malaysia. Email: sofinatamam@usim.edu.my

not only sitting on a comfortable chair, but also allowing them to have mobility [9]. The portability and adaptability of the EEG make it well-suited for investigating diverse elements of brain activity and connectivity in BCI, including motor imagery (MI). BCI can be classified into active, passive and reactive. MI is an active BCI, whereby the user intentionally generates specific brain signals to interact with an external device by executing imaginary movements without physically performing them [10].

MI-BCI is a beneficial technique that has been applied successfully for rehabilitation, gaming and device control. The most typical movements or commands used in MI tasks as control mechanisms for wheelchairs and cursors are left, right, forward, up and down [11]. MI-BCI activity is generated in two different rhythms (8–13 Hz and 13–30 Hz) [12]-[13]. When developing a BCI system, it is important to consider the number of sensors that can accurately record and resolve the signal's reliability [14]. It is also associated with user comfort. Multi-channel EEG data could achieve high classification accuracy (CA). However, it has increased the complexity and setup time of the experimental procedure [5]. For daily-time usage, a smaller number of EEG channels is more practical, but there are still limitations with reliability and low accuracy [15]. Gaur et al. [16] employed two public datasets to investigate the performance of reducing the number of channels. They discovered that by reducing the number of channels from 118 to 13, they were able to reach an accuracy of 80.56% in the BCI implementation. The person, as well as the well-designed experimental settings and classification algorithm, have a significant impact on the number of channels required for a high accuracy rate [17]. Thus, if high-accuracy classification can be obtained with only one EEG channel, it will be easier and more comfortable to use BCIs on a regular basis [18]. Extracting meaningful and relevant features from a single-channel EEG signal could be more challenging than from a multi-channel system. Due to limited dimensionality and information content across various brain regions, this may result in low accuracy and interpretability. Therefore, the feature extraction method is very important for getting sufficient CA for the EEG signals that come from one channel.

Therefore, this study proposes the fusion of a discrete wavelet transform (DWT)-based and time-domain feature extraction to improve the interpretation of movement tasks in single-channel EEG signals. The DWT decomposes the signal into different frequency components, enabling the analysis of a wide range of temporal and frequency characteristics within the same signal. Selected specific frequency components are used for relevant features extraction. Fusion of features integrates different sets of features captured from a single-channel EEG signal, providing a more comprehensive representation of the signal with useful data. The study investigates the impact of this feature-extraction approach on the performance of specific EEG channels.

The EEG signal from the following channels: Fp1, Fp2 and AF3 presented sufficient CA in the previous studies [18][19][20]. Besides that, it was reported that AF3 and AF4 are among the most informative channels found in two benchmark datasets [21]. According to previous research, it was found that there was significant activation in the prefrontal region in implementing MI tasks, making it plays an important role in MI tasks, including those related to gait and lower limb movement [22]-[23]. The region is involved in various cognitive and executive functions. Based on the findings of [24], it was suggested that MI depends greatly on executive resources, because tasks involving executive processes, such as calculations, have a significant impact on MI, but have a lesser effect on overt actions. Therefore, the study explores the potential of four channels located at the frontal right and left hemispheres of the forehead (Fp1, Fp2, AF3 and AF4) for implementing the MI. The position of the channels was considered to have the potential to enhance the practicality of the MI-BCI system [18]. Furthermore, the most employed channels for MI involving the hands and feet, specifically C3, C4 and Cz, are examined as well for the purpose of comparison. Foot movements should be observed around the Cz channel [25].

To achieve the aim of the study, three feature-extraction approaches are applied to two benchmark datasets, resulting in three feature sets: time-frequency features (DWT-based), time-domain features and fusion of DWT-based and time-domain features. Three classifiers are utilized to classify the selected features. They are Support Vector Machine (SVM), Logistic Regression (LR) and Naïve Bayes (NB).

2. RELATED WORKS

For multichannel feature extraction, Common Spatial Pattern (CSP) is commonly used [26]. Among all feature extraction techniques studied by Selim et al. [27], CSP produced excellent results when measuring accuracy and execution time. It is frequency-domain feature extraction that requires more channels for MI signal processing. Therefore, the time-frequency domain decomposition method is introduced for single-channel EEG signal execution. Short-time Fourier transforms (STFTs) are one of the time-frequency domain methods that were used in previous studies [21], [28][29][30]. However, STFT is not suitable for non-stationary applications because of the fixed window size [31]-[32]. Tiwari [21] introduced a novel Logistic S-shaped Binary Jaya Optimization Algorithm (LS-BJOA) for MI classification in BCI, while the Regularized Common Spatial Pattern (RCSP) was applied for feature extraction. The study validated its method on three public EEG datasets, achieving the CA of 83.59%, 82.09% and 89.02% on these datasets, respectively, with a reduced number of channels compared to baseline methods. In the single EEG channel research conducted by Chen et al. [30], it was reported that the FitzHugh-Nagumo (FHN)-PSD system achieved an average CA of 67.06% ± 8.73%, specifically on the C4 channel. The FHN-PSD system exhibited a 2.29% improvement over the FHN-STFTCSP approach, indicating its greater effectiveness in classifying EEG signals.

Through most of the datasets utilized for the comparison study, Wavelet Transform (WT) showed more robustness than CSP and power spectral density (PSD), as reported by Moumgiakmas and Papakostas [26]. This could be seen from the previous works implementing decomposition method in their studies. Three different signal-decomposition algorithms for MI-BCI systems were tested and compared. It was found that wavelet packet decomposition (WPD) was the most accurate method (92.8%). It was followed by the discrete wavelet transform (DWT) and empirical mode decomposition (EMD) [33]. The research indicates that the efficacy of their methodology can be improved by carefully choosing a suitable decomposition method and features, even with the small number of EEG channels (C3, C4 and Cz). WPD was used for decomposing the EEG signal to apply a hybrid feature set that combined it with the time-domain feature set [34]. However, results showed that the smallest number of channels (C3, Cz and C4) obtained the lowest CA, while using eighteen channels resulted in the highest mean CA of 91.1% for the BCI Competition III dataset IVa. The hybrid feature selection played an important role in the research to select the relevant features to be classified by SVM. In the studies of Ji et al. [35], two stages of the decomposition approach were applied. The EEG signal was decomposed using DWT to generate a narrow-band signal. The second decomposition method, EMD, was used to obtain a more concentrated signal for frequency-band signals. In order to improve the classification, an approximate entropy was determined. Rather than using DWT alone, this approach provides an additional method for extracting movement imagining signal features from two EEG channels (C3 and C4). The accuracy was 95.1% using SVM. However, the statistics of the approximate entropy were inconsistent. The tunable Q wavelet transform (TQWT) is a discrete-time WT that has been parametrized and has a tunable quality factor. The quality factor (Q), the redundancy rate (r) and the level of decomposition (L) are required as the basis functions for the decomposition. It was employed in the research conducted by Khare et al. [20]. The highest accuracy of 99.78% was achieved with the least squares support vector machine (LS-SVM) model. The selection of the most informative channels from a total of 118 was a critical aspect of the study, aimed at reducing computational load. However, despite the optimization, the multichannel setup is still required, which is too time-consuming to feasibly be deployed on the scalp every day.

In different applications, DWT was employed to extract the features, since it is an effective approach in terms of accuracy compared to other methods for categorizing epileptic cases based on the EEG. The combination of DWT with differential evaluation (DE) enhanced the classification result [36]. A promising result was achieved in the seizure identification by the concatenation of a feature matrix derived from DWT and EMD across multi and single-channel EEG recordings [37]. Instead of employing only DWT, the concatenation increased the accuracy of the single-channel EEG signals from 85% to 100%. Some EEG channels in the MI-BCI system worked better when DWT was combined with other feature extraction methods, as in the earlier research. This approach also enhanced the performance of single-channel EEG signals across different applications, which may benefit MI application.

3. METHODOLOGY

The methodology is divided into four phases: dataset acquisition, data preprocessing, feature extraction and selection and classification. The block diagram of the proposed approach is shown in Figure 1.

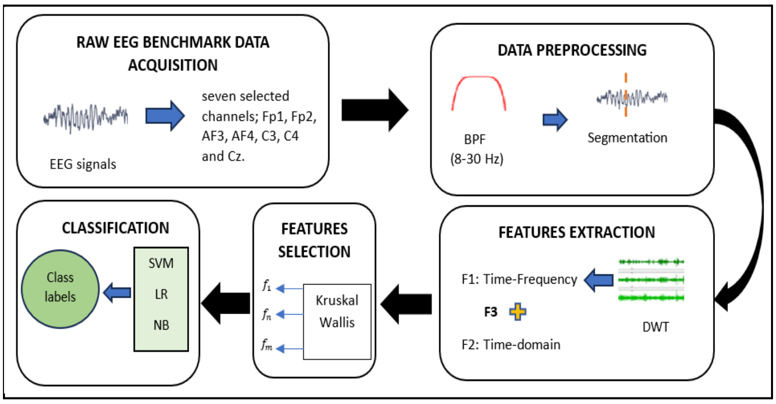

Figure 1. A block diagram of the proposed approach.

In the feature extraction phase, let the features in the first experiment be F1= $\{f_1,\ldots\ldots\ldots, f_n\}$, while the features in the second experiment is F2= $\{f_1,\ldots\ldots\ldots, f_m\}$. The features for the third experiment are therefore formally represented by:

$$\text{F3}= \{f_1,\ldots\ldots\ldots, f_n, f_{n+1},\ldots\ldots\ldots, f_m\} \tag{1}$$

where f_n represents different features in F1, f_m represents different features in F2 and F3 is the fusion features of F1 and F2. All phases are described in detail in the following sub-sections.

3.1 Motor Imagery (MI) Dataset Acquisition

Dataset 1 is the BCI Competition III (IVa) dataset [38]. It is the cued MI data with two tasks that was recorded using the extended 10-20 international system's 118 EEG channels. It was from five healthy participants (*aa*, *al*, *av*, *aw* and *ay*) who comfortably sat during the experiment. The MI tasks were completed by conducting 140 trials of MI tasks with the right-hand (*rh*) movement and 140 trials with the right-foot (*rf*) movement. The total number of trials for each participant was 280. They were each provided with a 3.5-second visual stimulus. The dataset was collected at a sampling rate of 1000 Hz. However, they were down-sampled to 100 Hz for analysis purposes.

Dataset 2 is the OpenBMI dataset which comprises data collected from 54 healthy individuals [39]. The experiment recorded binary MI tasks of the right (*rh*) and left (*lh*) hands. Each trial started with a preparation phase, followed by MI tasks for a duration of 4 seconds once a visual cue was displayed. The experiment had four different stages with 100 trials each, equally split between right- and left-hand imagery. For this study, 19 participants (S1, S2, S3, S9, S18, S19, S21, S22, S28, S29, S30, S32, S33, S36, S37, S43, S44, S45 and S52) with proven MI-BCI literacy were selected. The data was analyzed using offline EEG data from the first session [39]. EEG signals were recorded at 1000 Hz over 62 channels, but down-sampled to 100 Hz for analysis.

C3, Cz and C4 channels are extensively employed for analysis in MI studies, regardless of whether they are multi-EEG channel or single-EEG channel analysis. The channels' location is over the primary motor cortex areas of the brain for controlling voluntary movements. C3 and C4 are located over the left and right hemispheres, respectively, and are known to capture important MI properties [30], [40]. The Fp2 channel, which is located on the forehead, was reported to have equivalent high CA to C4 by Ge et al. [18]. Furthermore, in the previous study, the AF3 and AF4 channels, located near the forehead, were identified as the channels providing the most relevant information [19], [21]. The Laplacian score for channel selection demonstrated that Fp1 was also identified as the most informative channel [20]. Thus, among the 118 channels in Dataset 1 and the 62 channels in Dataset 2, only the EEG signals from the following channels are selected for subsequent processing and analysis: C3, Cz, C4, Fp1, Fp2, AF3 and AF4.

3.2 Data Preprocessing

The preprocessing phase is essential for obtaining reliable data that is ready for meaningful interpretation about brain activity. It filters out any artifacts and noise in the signal, allowing useful features to be extracted from the raw data. Two EEG frequency sub-bands, α (8-13 Hz) and β (13-30 Hz), needed to be isolated from other ranges of the raw EEG signal. The frequency bands are associated with the motor activation, preparation and planning of imagery movement [41]. Therefore, the 5th-order Butterworth filter with a pass band of 8- 30 Hz was employed in the first step, as implemented in previous works [19], [39]. After that, the signals were segmented to extract the dataset's epochs with a window length of 3 seconds (0.5 s to 3.5 s) for Dataset 1 and 2.5 seconds (1s to 3.5s) for Dataset 2. They were prepared to extract relevant features that can distinguish between two MI tasks.

3.3 Feature Extraction

In the feature-extraction phase, three experiments were conducted. F1 involved the DWT decomposition technique to process single-channel EEG. The technique enables the separation of a single-component signal into multiple sub-signals. Each component corresponds to a different part in a specific frequency band of the signal that is essential for feature extraction. It is possible to efficiently extract relevant information or features from a complex signal that are beneficial for task classification. Down samplers and consecutive high- pass (g_n) and low-pass (h_n) filtering of the time series are used in the DWT decomposition of the input signal (x_n), as shown in Figure 2. It split the signal into high-frequency and low-frequency content in the form of detail and an approximate coefficient [42]. For a further level of decomposition, only the approximations are passed again through the low-pass and high-pass filters. In this study, signals were decomposed using three levels of DWT with the Daubechies 4 wavelet (db4) [35], resulting in three detailed components (D1, D2 and D3) and one approximation component (A3), as shown in Figure 2. The frequency range for each selected band is shown in Table 1.

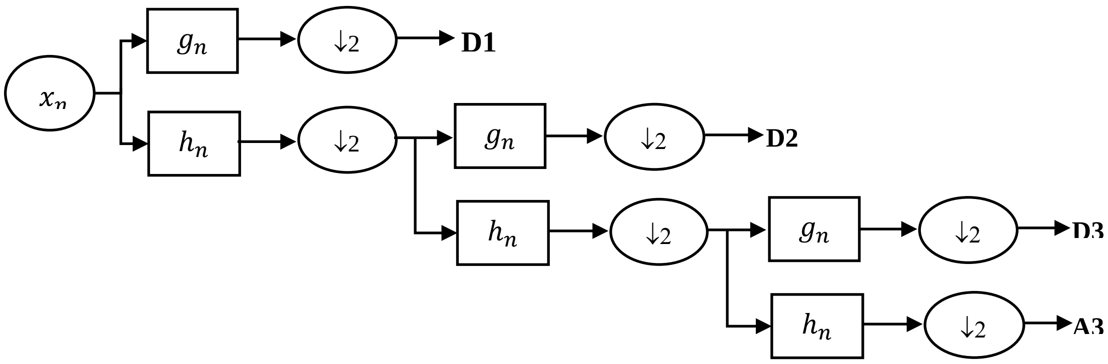

Figure 2. DWT decomposition of the input signal.

Table 1. Decomposition levels, coefficient vectors and their frequency ranges.

Level	Coefficient Vector	Frequency Range (Hz)
1	D1	25-50
2	D2	12.5-25
3	D3	6.25-12.5

As A3's frequency range (0- 6.25 Hz) is outside the required frequency band, it was excluded for feature extraction. Moreover, the frequency of a signal that is less than 5 Hz may have artifacts [35]. D1 was included in the analysis, because it might still offer a useful filtered signal that is relevant to the specific frequency of interest, which is 25 to 30 Hz. As a result, five features were extracted from each detail component, yielding a total of fifteen (15) features in F1. The feature in each sub-band is represented by $F1_{D1} = \{\mu_1, \sigma_1,\ skewness_1, kurtosis_1, P_{av\ 1}\}$ for D1.
D2 is represented by $F1_{D2} = \{\mu_2, \sigma_2,\ skewness_2, kurtosis_2, P_{av\ 2}\}$, while D3 is represented by $F1_{D3} = \{\mu_3, \sigma_3,\ skewness_3, kurtosis_3, P_{av\ 3}\}$. The equations of the features in F1 are as follows:

The absolute mean (μ)is defined as [33]:

$$\mu = \frac{1}{N}\sum_{n=1}^{N} |y_n| \tag{2}$$

The standard deviation (σ) is defined as [37]:

$$\sigma = \sqrt{\frac{1}{N}\sum_{n=1}^{N}(y_n - \bar{y})^2} \tag{3}$$

The skewness is defined as [37]:

$$skewness = \frac{1}{N}\frac{\sum_{n=1}^{N}(y_n - \bar{y})^3}{\sigma^3} \quad (4)$$

The kurtosis is defined as [37]:

$$kurtosis = \frac{1}{N}\frac{\sum_{n=1}^{N}(y_n - \bar{y})^4}{\sigma^4} \quad (5)$$

The average power (P_{av}) is defined as [33]:

$$P_{av} = \sqrt{\frac{1}{N}\sum_{n=1}^{N} {y_n}^2} \quad (6)$$

where N is the number of samples, y_n is the signal in each sub-band, $\bar{y}$ is the mean of the signal in each sub-band and n is an integer that belongs to 1 to N.

Eight time-domain features were directly extracted from the processed signal in F2. These include the mean absolute value, Root Mean Square (RMS), Hjorth parameters (activity, mobility and complexity), waveform duration, skewness and kurtosis represented by F2 $= \{\mu, RMS, Activity, Mobility, Complexity, WL, skewness, kurtosis\}$. The equations for the parameters are as follows:

The mean absolute (μ) value is written as [33] :

$$\mu = \frac{1}{T}\sum_{t=1}^{T} |x_t| \quad (7)$$

RMS is the square root of the average of the signal's squared value in the time domain. The RMS is written as [43]:

$$RMS = \sqrt{\frac{1}{T}\sum_{t=1}^{T} x_t^2} \quad (8)$$

The amplitude variance of signal samples is used to calculate the Hjorth activity that is written as [44]-[45]:

$$Activity = var\ (x_t) \quad (9)$$

The frequency's mean approximation is determined by the Hjorth mobility that is written as [44]-[45]:

$$Mobility = \sqrt{\frac{var(x_t')}{var\ (x_t)}} \quad (10)$$

The power spectrum's standard deviation is determined by Hjorth complexity that is written as [44], [45]:

$$Complexity = \frac{Mobility(x_t')}{Mobility\ (x_t)} \quad (11)$$

Waveform length (WL) represents the cumulative absolute difference between adjacent samples and provides a measure of the signal's overall variation. It can be written as follows [46]:

$$WL = \sum_{t}^{T} |x_t - x_{t-1}| \quad (12)$$

The skewness is written as [37]:

$$skewness = \frac{1}{T}\frac{\sum_{n=1}^{N}(x_t - \bar{x})^3}{\sigma^3} \quad (13)$$

The kurtosis is written as [37]:

$$kurtosis = \frac{1}{T}\frac{\sum_{n=1}^{N}(x_t - \bar{x})^4}{\sigma^4} \quad (14)$$

where T is the number of samples, $x_t$is the processed signal, x_t' is the first derivative of the signal sample x_t, $var\ (x_t)$ is the variance of the signal sample x_t, $\bar{x}$ is the mean of the signal and t is an integer that belongs to 1 to T.

In F3, all features in F1 and F2 were combined and represented as F3 = $F1_{D1} \cup F1_{D2} \cup F1_{D3} \cup F2$ with twenty-three (23) features in total. The Kruskal-Wallis test was applied to select the features of F3 that have a p-value of less than 0.05. F3 in combination with the feature selection is represented as FS. The approach enables us to consider the unique features of both sets, providing a more comprehensive analysis. The features were evaluated and analyzed to investigate the enhancement to the classification performance.

3.4 Classification

The SVM classifier is one of the most frequently used methods for MI task classification. The SVM aims to accomplish both accurate classification and robust generalization by maximizing machine performance while minimizing the complexity of the learned model [47]. The SVM identifies the hyperplane that maximizes the margin between different classes of data points. The margin is the distance between the hyperplane and the nearest data points from each class. This is also known as support vectors. SVMs sometimes give a better fit and are computationally more efficient [48].

The LR has a low risk of overfitting, because the model complexity is minimal [49]. It determines a relationship between a single or a set of independent variables (features) and the likelihood that the dependent variable will fall into a specific class. In the LR, the result always falls between 0 and 1 by using the logistic function representing the estimated probability of the positive class. Based on the probability, the LR model creates a decision boundary that separates the two classes. During training, the method changes the model's parameters to reduce the difference between the predicted probability and the actual binary labels in the training data. The data points near the margin have significantly less influence due to the logit transform [48].

Naïve Bayes (NB) is useful when most or all the predictor variables are also binary or categorical. Given the class label, the assumption in the NB is that all features are conditionally independent and this simplifies the modeling process [50]. The NB can also be applied in situations where there are three or more possible outcomes. The strategy in this case is to determine the probabilities of each possible outcome before selecting the one with the highest probability. However, rather than being highly precise values, the estimated probabilities should be considered approximation figures when the assumption of conditional independence is violated [48]. The NB classification algorithm has demonstrated high CA when applied to a limited sample dataset utilizing the Poisson distribution model [50].

Performance was evaluated by the CA and F1-score. The accuracy is defined as the ratio of correctly identified samples or observations to the total number of input samples in the same class. It describes the classifier's effectiveness in performing its tasks successfully. The F1-score is a metric that balances both precision and recall. The equations are written as [51]:

$$Accuracy = \frac{TP+TN}{TN+TP+FN+FP} \times 100\% \tag{15}$$

$$F1_{score} = \frac{2TP}{2TP+FP+FN} \tag{16}$$

where true positive (TP) refers to the trials in the experiment that are correctly labelled as positive. The term "TN" refers to true negatives, which represent the number of trials correctly classified as negative, while “FP” is false positive representing the trials incorrectly classified as positive and “FN” is false negative when the trials are incorrectly classified as negative.

By preventing over-fitting, the cross-validation approach enhances model efficiency. The performance parameters were evaluated using a ten-fold cross-validation approach. A ten-fold cross-validation of results divides features into ten segments or folds of a similar scale. It consists of nine training sets and one testing set, whereby the model is trained in each round with the training sets and evaluated using one testing set. The average accuracy is computed with ten rounds of the process. The classification is implemented using MATLAB R2022a.

4. RESULTS

This section consists of two sub-sections. The first sub-section discusses the classification-performance result obtained by combining the feature vectors of all participants. The second sub-section focuses on the classification performance of the FS across all the participants and channels.

4.1 Performance Evaluation of All Participants

Figure 3 shows the CA of MI tasks when the features vectors of all participants in the Dataset 1 were combined. The accuracy of all channels is less than 70%, possibly due to significant inter-individual variability in brain signals, including cognitive ability and activity patterns, that has an impact on overall performance [16]. Employing F3 without FS along with Support Vector Machines (SVMs) has been shown to improve the CA of EEG signals, specifically from AF4, C3 and Cz, as shown in Figure 3(a).

On the other hand, the implementation of FS led to a decrease in the CA for AF4 and C3, while Cz, Fp1, AF3 and C4 showed an improvement in the CA. This implies that FS had a different impact on the various channels, potentially due to the specific features that were chosen and their significance according to the classification task. Figure 3(b) shows that F3 with LR also resulted in positive results for enhancing the CA of Cz. Furthermore, FS resulted in further improvement in the CA of Cz. It indicates that applying FS, along with LR, can be a beneficial approach for getting a higher CA of Cz. Furthermore, FS led to higher CA, not only for Cz, but also for other channels, such as Fp1, AF3 and C4, as shown in Figure 3(c). The figure also illustrates the lack of CA improvement when combining F3 with the NB classifier. This indicates that the interaction between F3 and NB, as well as FS and NB, did not enhance the CA. It emphasizes the incompatibility of using F3 and FS together with NB. In overall, C3 has higher CA across all classifiers.

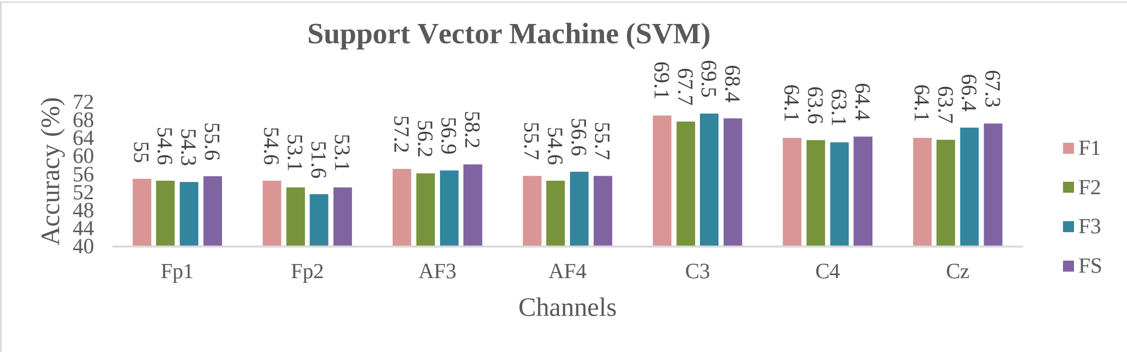

(a)

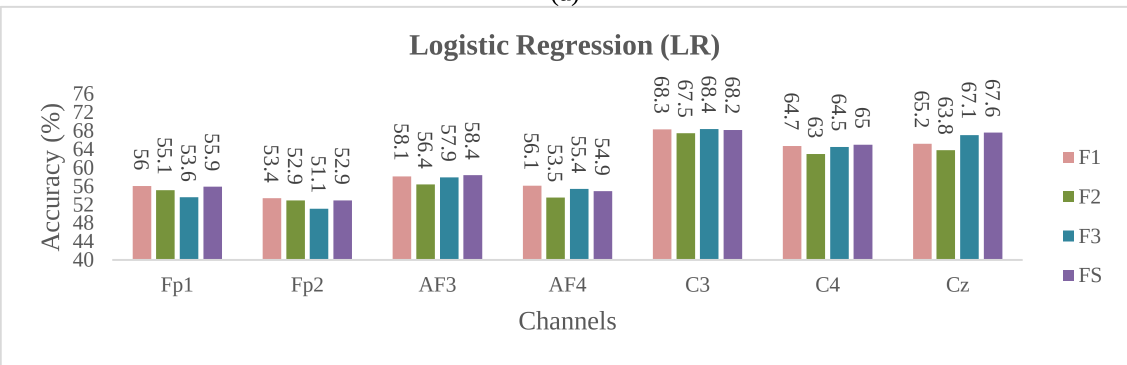

(b)

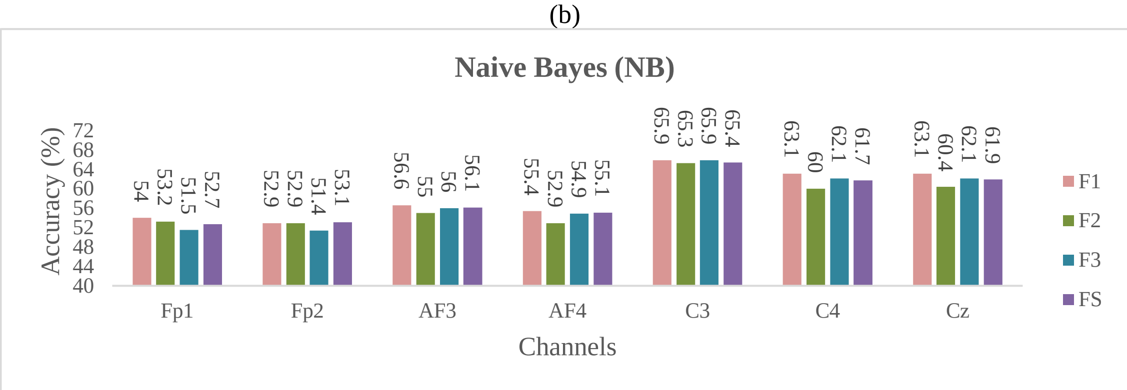

(c)

Figure 3. Dataset 1 classification accuracy (%) comparison across experiments and channels using a) SVM, b) LR and c) NB.

A statistical analysis was applied to determine whether there are statistically significant differences in the CA between three different classifiers in separate experiments using Dataset 1. Due to the small sample size, the Friedman test was conducted. The findings demonstrated a statistically significant difference in the accuracy of the classifiers when assessed using feature sets F1, F2 and F3. This was shown by the p-value of 0.004, 0.008 and 0.018, respectively. This suggests that the selection of a classifier, when used in conjunction with the features from F1, F2 or F3, significantly affects the CA. In contrast, the use of classifiers based on the feature set of FS did not have a significant effect on the CA. This is supported by a p-value of 0.104, which is higher than 0.05.

Figure 4 shows the CA of MI tasks when the feature vectors of nineteen participants in Dataset 2 were combined. The accuracy of all channels is also less than 70%, possibly due to significant inter-individual variability in brain signals that have an impact on the overall performance [16]. Figure 4(a) depicts that employing F3 in the absence of FS in conjunction with Support Vector Machines (SVM) has demonstrated its effectiveness in improving the CA of EEG signals, specifically from Fp2, C4 and Cz. On the other hand, the implementation of FS led to an increase in the CA for C3. Figure 4(b) shows that F3 with LR also resulted in positive results for enhancing the CA of C4, Cz and AF4. Furthermore, FS resulted in higher CA, not only for Fp2, but also for other channels; AF4 and C3. FS resulted in further improvement in the CA of AF4. Figure 4(c) illustrates the positive results in terms of CA improvement of Fp1, C3, C4 and Cz resulting from the combination of F3 and NB. The interaction between F3 and NB, as well as FS and NB, did not result in an improvement of AF3. It shows that F2 resulted in higher CA for AF3 compared to F3 and FS.

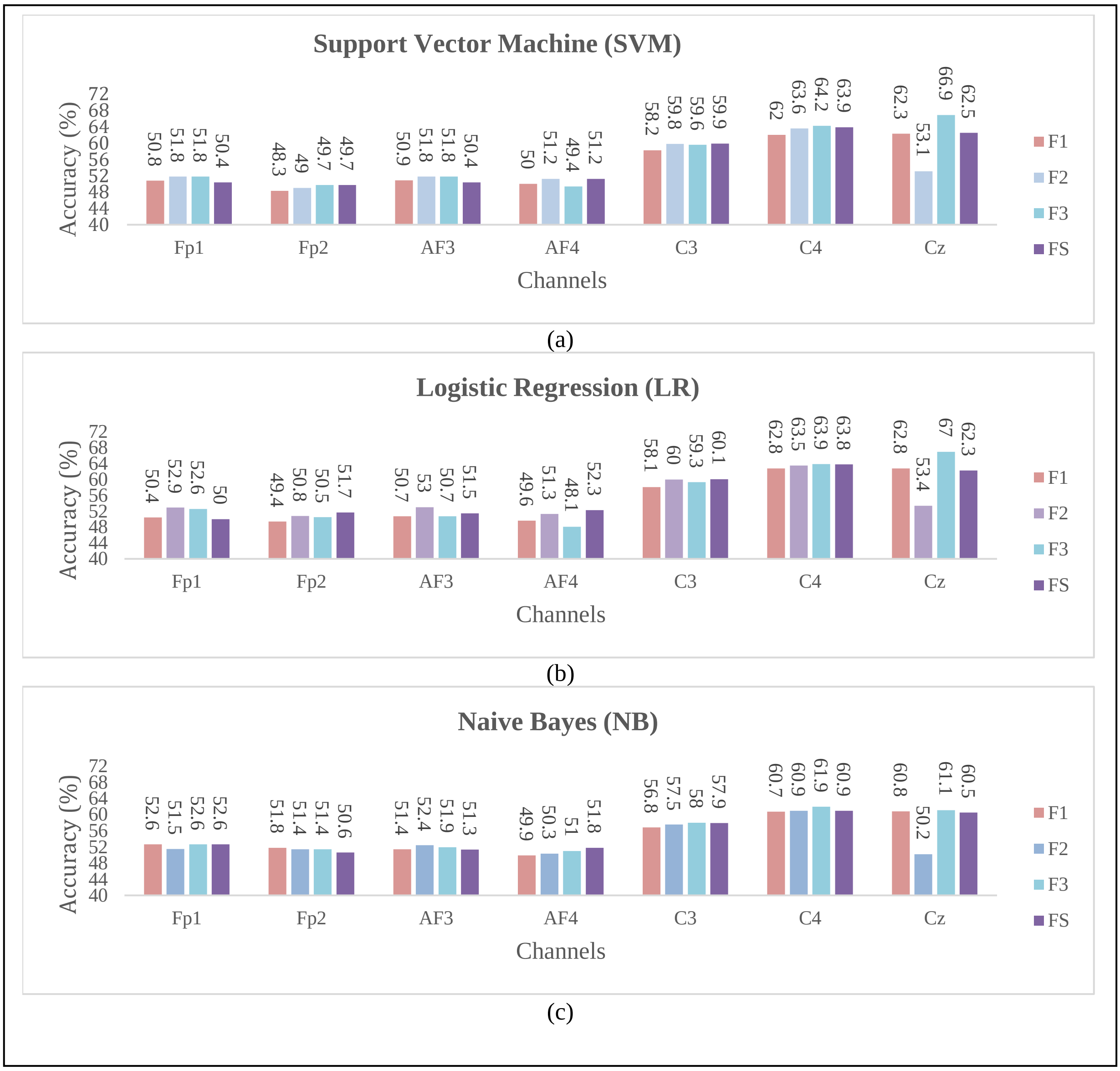

Figure 4. Dataset 2 classification accuracy (%) comparison across experiments and channels using a) SVM, b) LR and c) NB.

A statistical analysis was applied to determine whether there are statistically significant differences in the CA between three different classifiers in separate experiments using Dataset 2. The Friedman test revealed no significant difference in the accuracy of the classifiers across feature sets F1, F3 and FS. This was shown by a p-value exceeding 0.05. This suggests that the selection of a classifier, when applied with F1, F3 and FS, does not significantly affect the CA. In contrast, classifiers using the F2 feature set significantly impact the CA as indicated by a p-value of 0.05.

Table 2 presents F1-scores for *rh* and *rf* in Dataset 1 and *rh* and *lh* in Dataset 2 across the channels and classifiers. The results show that *rh* generally has higher scores than *rf* and *lh*, indicating better classifier performance for *rh* tasks. This suggests that the features are more distinct and easier to identify. It is important to note that the F1-score obtained from the combination of feature vectors for all participants can vary due to the variation in participants' abilities in the MI tasks. There are challenges in classifying either *rf* or *lh* tasks, as seen in varied F1-scores except for C4 and Cz in Dataset 2. It can be associated with features and data patterns of *lh* that are more dominant and easier to recognize. This highlights the importance optimizing the feature extraction or selection approach for improving the CA. In the previous study utilizing the same dataset as Dataset 1, it was also observed that *rh* exhibited a higher accuracy compared to *rf* when employing the WPD- k-NN method [33].

Table 2. $F1_{score}$ (%) of FS for Dataset 1 and Dataset 2.

CHN	**Dataset 1**						**Dataset 2**					
	SVM		**LR**		**NB**		**SVM**		**LR**		**NB**	
	rh	***rf***	***rh***	***rf***	***rh***	***rf***	***rh***	***lh***	***rh***	***lh***	***rh***	***lh***
Fp1	59.1	51.6	57.5	54.17	60.6	40.9	63.1	24.3	57.8	38.6	63.4	32.8
Fp2	57.9	47.3	55.2	50.33	60.8	41.5	64.7	12.5	58.8	41.7	62.3	28.1
AF3	58.9	57.5	59.1	57.70	55.6	56.5	62.3	27.7	56.9	44.6	61.8	62.4
AF4	58.3	52.8	56.5	53.23	58.6	51.1	55.2	46.4	54.0	50.5	57.4	44.4
C3	68.2	68.5	67.9	68.49	67.4	63.3	61.6	58.1	60.6	59.6	64.2	48.9
C4	64.8	63.9	65.6	64.43	63.4	59.9	62.3	65.3	62.9	64.6	53.2	66.4
Cz	67.8	66.4	68.2	67.08	63.1	60.5	58.8	65.7	59.8	64.5	52.7	66.1

4.2 Performance Evaluation of Individual Participants

The CA for each participant was determined by classifying features that were selected through the feature-selection process (FS). They were analyzed to get a more in-depth study of the proposed technique, as shown in Table 3. The CA exceeding 70% is presented in boldface.

In Dataset 1, noteworthy results were achieved with different classifiers. When employing the SVM, *aw* achieved the highest CA at 81.4% by utilizing commonly employed channels, demonstrating the robustness of the SVM in capturing neural patterns related to MI. In addition, the channel on the forehead had the highest CA at 63.6%. It was performed by *aw* with AF4. Switching to the LR as the classifier, *al* achieved the CA of 87.5% via C3 which represents the highest CA obtained for the dataset. *al* also demonstrated the CA of 62.1%, specifically from AF4. The NB achieves a maximum CA of 79.3% when using the C3 channel. The highest achievable accuracy for the forehead channel is 60%, specifically from the AF3 channel. The results are in line with the finding in [21], where AF4 was identified as one of the most informative channels for *aw* and both AF3 and AF4 for *al*.

In Dataset 2, S36 gets the maximum CA of 93% by classifying the features of C4 using the SVM. S36 outperformed other participants with features from both C4 and Cz channels across all classifiers. When examining the channels on the forehead (Fp1 and AF3), S29 demonstrated great performance compared to other participants. The CA for S29 exceeded 70% and reached up to 86% across all classifiers, which is sufficient for BCI. There are participants getting higher CA on the channels that are located on the forehead compared to the channels that are commonly used for MI. This is demonstrated by S28 and S29 with SVM. For example, the CA of AF4 (64%) is higher than that of C3 (51%) and C4 (58%), while S29 has a higher CA of Fp1 (86%) and AF3 (77%) compared to the CA of C3 (70%), C4 (60%) and Cz (59%).

Table 3. The minimum and maximum values of CA across classifiers and channels.

Dataset	**Classifier**	**Level**	**Channels**						
			Fp1	**Fp2**	**AF3**	**AF4**	**C3**	**C4**	**Cz**
Dataset 1	SVM	Min	50.7 (*av*)	52.1 (*aa*)	48.2 (*aa*)	56.1 (*aw*)	52.1 (*ay*)	52.1 (*ay*)	53.7 (*ay*)
		Max	61.8 (*al*)	58.6 (*al*)	60.7 (*al*)	63.6 (*aw*)	**81.4 (*aw*)**	**81.4 (*aw*)**	**79.3 (*aw*)**
	LR	Min	51.1 (*av*)	50.4 (*av*)	52.1 (*av*)	53.2 (*aw*)	55.4 (av)	54.3 (ay)	55.7 (ay)
		Max	57.5 (al)	58.2 (*aw*)	59.6 (*aw*)	62.1 (*al*)	**87.5 (*al*)**	**80.7 (*aw*)**	**79.3 (*aw*)**
	NB	Min	52.1 (*ay*)	50.4 (*aa*)	53.2 (*aa*)	55.4 (*aa*)	55.7 (aw)	57.9 (ay)	55 (ay)
		Max	56.1 (*al*)	56.1 (*ay*)	60.0 (*al*)	58.9 (*al*)	**79.3 (*al*)**	**73.2 (*aw*)**	**74.3 (*aw*)**
Dataset 2	SVM	Min	45.00 (S32,S33 &S44)	38.00 (S32)	42.00 (S9)	33 (S32)	40.00 (S1)	40.00 (S2)	41.00 (S2)
		Max	**86 (S29)**	63.00 (S3&S22)	**77 (S29)**	64 (S28)	**75 (S44)**	**93 (S36)**	**91.00 (S36)**
	LR	Min	41 (S44)	37 (S5)	37 (S2)	42 (S1&S32)	45 (S19)	45 (S5)	40 (S1)
		Max	**78 (S29)**	66 (S3)	**73 (S29)**	67 (S29)	**73 (S37)**	**86 (S36)**	**85 (S36)**
	NB	Min	44 (S36)	39 (S5)	38 (S2)	36 (S52)	43 (S1)	44 (S2)	38 (S2)
		Max	**81 (S29)**	64 (S18)	**72 (S29)**	63 (S18)	**75 (S44)**	**88 (S36)**	**85 (S36)**

5. DISCUSSION

Based on the result of combining the feature vectors of all participants, C3 and C4 exhibit the highest CA across all classifiers for Dataset 1 and Dataset 2, respectively. C3 and C4 were used a lot in past studies, because they are placed over the motor cortex of the brain and can record unique patterns during MI activities [30], [35], [40]. The SVM and LR produce comparable results, because each model uses all data points, with points closer to the margin having considerably less impact [48]. The F3 features, extracted from EEG signals across both datasets, could provide relevant information for classification. Further improvement in the CA is also possible with feature selection. This suggests that by selecting relevant features with an appropriate classifier, the CA could be greatly improved. Further exploration might also expand the potential of Fp1, AF3 and AF4 channels for a single-channel execution in MI. Moreover, the positioning of the AF3 and AF4 channels on the forehead, away from the eyes, could offer practical advantages by minimizing the direct impact of eye blinks compared to Fp1 and Fp2.

Regarding the performance of individual participants, the study demonstrated that the commonly employed channels consistently achieved accuracy levels exceeding 70% across different classifiers using the proposed approach in both datasets. The threshold of 70% is generally recognized as meeting the requirements needed for effective BCI implementation. This indicates the practicality and reliability of the proposed approach for BCI applications [39]. AF3 and AF4 showed the potential for use in the single-channel BCI execution, as they frequently exhibited accuracies higher than 60% with the proposed approach. This is also considered as BCI literacy threshold determined in the previous MI study [52]. Further exploration could strengthen the practicality and reliability of a single-channel BCI systems for broader implementation in real-world applications. Moreover, S29 offers the CA that is comparable to the common channels. Despite the recognition of C3 and C4 as the channels that offer superior MI features [40], there are participants achieving higher CA using channels other than C3 or C4 [18][19][20]. The example is shown by S28 and S29 by using SVM as the classifier. It is strongly affected by the involvement of participant, as well as the well-designed experimental conditions and the implementation of an effective classification algorithm [17], [21].

Table 4 presents several existing techniques employed on the Dataset 1. For any of the five subjects, the proposed approach does not provide the best CA. Most of the past research used more than two channels to get more relevant information or features, resulting in high CA. The study conducted by Khare and

Bajaj [19] successfully obtained very high CA. However, they have different approaches to select the best single channel for further processing. They were using multi-cluster unsupervised learning channel selection (MCCS) to rank or find the best single channel from the 118 channels in the BCI system. Even though they are using the same dataset, the most informative channel was different when they used different methods for channel selection [20]. For Dataset 2, the CA is compared with the CA from the first session of the previous study [39] with the same participants. The technique compared include the 10-fold cross validation with the CSP (CSP-cv) and Linear Discriminant Analysis (LDA) as the classifier. They employed 20 channels that are in the motor cortex region for the analysis. The average of the CA for 19 participants is 87.14±9.14 which is 33.85% greater than the average of the CA in AF4 (53.29±9.12) and 22.43% higher than the average of the CA in C4 (64.71±11.49). S33 achieves the highest CA of 98.1%. For this study, the highest CA is 93% which is 4.9% lower than S33. Even though the overall performance is not comparable to the previous work, the CA for certain participants is relatively promising when consider the number of channels.

Table 4. A comparison of the CA for Dataset 1 across different participants.

Author(s)	**Approach**	**No. of channels**	***aa***	***al***	***av***	***aw***	***ay***	**Average ± std.**
Selim et al. [27]	CSP\AM-BA-SVM	18	86.10	100	66.84	90.63	80.95	85.00± 12.29
Khare and Bajaj [19]	F-VMD\ F-ELM	1 (AF3)	100	100	100	100	100	100
Roy et al. [53]	HWE/ Decision Tree	16	100	87.50	100	71.87	100	91.87± 12.42
Tiwari [21]	LS-BJOA/ RCSP	In the bracket below the CA	89.34 (29)	94.08 (18)	80.54 (37)	93.5 (31)	87.68 (23)	89.02± 4.88 (27.6)
Gao et al. [54]	SR-TT/ SVM-RBF	118	84.64	91.07	82.50	87.50	81.07	85.36
Proposed approach	DWT and time domain features/ LR	1(C3)	60	**87.5**	55.4	60.4	76.4	67.94±13.52
		1 (AF4)	59.3	**62.1**	57.5	53.2	54.3	57.28±3.64

There are a few limitations to the proposed approach. Each participant's brain activity during MI might exhibit a unique pattern and variation. The approach might not be able to capture specific patterns from certain participants, including those who might be BCI illiterate. The applicability of Kruskal-Wallis for feature selection may be restricted for some individual participants. There is a possibility that the accuracy of the findings could decrease after selecting specific features, indicating the inconsistency of the selector in improving the performance of the classification. The selection could lead to the elimination of valuable information for certain participants, hence making the MI tasks difficult to interpret. The study is limited to the datasets of healthy participants. The results may differ when applied to a specific group of individuals with relevant health conditions.

6. CONCLUSION

In this study, the proposed approach was applied to Dataset 1 (BCI Competition III (IVa)) and Dataset 2 (OpenBMI) to evaluate the classification performance. The approach slightly increased the CA on certain channels with F3 and FS, compared to relying only on the DWT decomposition. While not all channels showed an increase in the CA for all participants, the CA of individual performance improved notably. Particularly, *al* reached up to 87.5% of CA on C3 by using LR and S36 achieved 93% of CA on the C4 channel. Additionally, participant S29 achieved sufficient CA on Fp1 and AF3 channels that is comparable to those of commonly used channels for MI. This suggests that the proposed approach, when combined with relevant features and appropriate classifiers, has the potential to improve overall classification performance. This extends its applicability to the forehead channels, necessitating further investigation of the channels in the context of our study. Although the proposed approach encounters difficulties in achieving high CA across participants, there is a room for improvement through comprehensive evaluation. Evaluating the effectiveness of the approach in different MI tasks and participant groups can aid in determining its strengths and limitations in various contexts. To optimize the classification performance, other feature-selection techniques, such as hybrid or wrapper methods, could be explored. Besides that, it would be valuable to conduct a comprehensive comparison between the proposed approach and the standard methods, such as the CSP technique, to identify their respective strengths and weaknesses.

REFERENCES

[1] J. L. Collinger et al., "Functional Priorities, Assistive Technology and Brain-Computer Interfaces After Spinal Cord Injury," J. of Rehabilitation Research and Development, vol. 50, no. 2, pp. 145–160, 2013.

[2] E. K. St. Louis, L. C. Frey and J. W. Britton, Electroencephalography (EEG): An Introductory Text and Atlas of Normal and Abnormal Findings in Adults, Children and Infants, Chicago: American Epilepsy Society; PMID: 27748095, 2016.

[3] L. Kauhanen et al., "EEG and MEG Brain-Computer Interface for Tetraplegic Patients," IEEE Transactions on Neural Systems and Rehabilitation Engineering, vol. 14, no. 2, pp. 190–193, Jun. 2006.

[4] N. Kulkarni and V. Bairagi, "Electroencephalogram and Its Use in Clinical Neuroscience," in Book: EEG-based Diagnosis of Alzheimer Disease, pp. 25–35, DOI: 10.1016/B978-0-12-815392-5.00002-2, 2018.

[5] J. Liao, J. Wang, C. A. Zhan and F. Yang, "Parameterized Aperiodic and Periodic Components of Single-channel EEG Enables Reliable Seizure Detection," Physical and Engineering Sciences in Medicine, DOI: 10.1007/s13246-023-01340-6, Sep. 2023.

[6] G. Kaushik, P. Gaur, R. R. Sharma and R. B. Pachori, "EEG Signal Based Seizure Detection Focused on Hjorth Parameters from Tunable-Q Wavelet Sub-bands," Biomed. Signal Process. Control, vol. 76, p. 103645, DOI: 10.1016/j.bspc.2022.103645, Jul. 2022.

[7] A. Babiker and I. Faye, "A Hybrid EMD-Wavelet EEG Feature Extraction Method for the Classification of Students' Interest in the Mathematics Classroom," Applied Computational Intelligence and Soft Computing, vol. 2021, pp. 1–8, DOI: 10.1155/2021/6617462, Jan. 2021.

[8] M. Zhong, Q. Yang, Y. Liu, B. Zhen, F. Zhao and B. Xie, "EEG Emotion Recognition Based on TQWT-features and Hybrid Convolutional Recurrent Neural Network," Biomed. Signal Process. Control, vol. 79, p. 104211, DOI: 10.1016/j.bspc.2022.104211, Jan. 2023.

[9] M. F. Mridha et al., "Brain-Computer Interface: Advancement and Challenges," Sensors, vol. 21, no. 17, p. 5746, DOI: 10.3390/s21175746, Aug. 2021.

[10] X. Gu et al., "EEG-based Brain-Computer Interfaces (BCIs): A Survey of Recent Studies on Signal Sensing Technologies and Computational Intelligence Approaches and Their Applications," IEEE/ACM Transactions on Computational Biology and Bioinformatics, vol. 18, no. 5, pp. 1645–1666, 2021.

[11] M. Rashid et al., "Current Status, Challenges and Possible Solutions of EEG-based Brain-computer Interface: A Comprehensive Review," Frontiers in Neurorobotics, vol. 14. Frontiers Media S.A., DOI: 10.3389/fnbot.2020.00025, Jun. 03, 2020.

[12] Jusas and Samuvel, "Classification of Motor Imagery Using a Combination of User-specific Band and Subject-specific Band for Brain-Computer Interface," Applied Sciences, vol. 9, no. 23, p. 4990, 2019.

[13] C. Neuper, M. Wörtz and G. Pfurtscheller, "ERD/ERS Patterns Reflecting Sensorimotor Activation and Deactivation," Progress in Brain Research, pp. 211–222, DOI: 10.1016/S0079-6123(06)59014-4, 2006.

[14] S. Saha et al., "Progress in Brain Computer Interface: Challenges and Opportunities," Frontiers in Systems Neuroscience, vol. 15, DOI: 10.3389/fnsys.2021.578875, Feb. 25, 2021.

[15] L. Brusini, F. Stival, F. Setti, E. Menegatti, G. Menegaz and S. F. Storti, "A Systematic Review on Motor-imagery Brain Connectivity-based Computer Interfaces," IEEE Transactions on Human-Machine Systems, vol. 51, no. 6, pp. 725–733, DOI: 10.1109/THMS.2021.3115094, Dec. 2021.

[16] P. Gaur, K. McCreadie, R. B. Pachori, H. Wang and G. Prasad, "An Automatic Subject Specific Channel Selection Method for Enhancing Motor Imagery Classification in EEG-BCI Using Correlation," Biomed Signal Process Control, vol. 68, p. 102574, DOI: 10.1016/j.bspc.2021.102574, Jul. 2021.

[17] L. Zhang and Q. Wei, "Channel Selection in Motor Imaginary-based Brain-Computer Interfaces: A Particle Swarm Optimization Algorithm," J. of Integrative Neuroscience, vol. 18, no. 2, pp. 141–152, DOI: 10.31083/j.jin.2019.02.17, 2019.

[18] S. Ge, R. Wang and D. Yu, "Classification of Four-class Motor Imagery Employing Single-channel Electroencephalography," PLoS One, vol. 9, no. 6, p. e98019, Jun. 2014.

[19] S. K. Khare and V. Bajaj, "A Facile and Flexible Motor Imagery Classification Using Electroencephalogram Signals," Computer Methods and Programs in Biomedicine, vol. 197, p. 105722, DOI: 10.1016/j.cmpb.2020.105722, Dec. 2020.

[20] S. K. Khare, N. Gaikwad and N. D. Bokde, "An Intelligent Motor Imagery Detection System Using Electroencephalography with Adaptive Wavelets," Sensors, vol. 22, no. 21, p. 8128, Oct. 2022.

[21] A. Tiwari, "A Logistic Binary Jaya Optimization-based Channel Selection Scheme for Motor-imagery Classification in Brain-Computer Interface," Expert Systems with Applications, vol. 223, p. 119921, DOI: 10.1016/j.eswa.2023.119921, Aug. 2023.

[22] K. Kotegawa, A. Yasumura and W. Teramoto, "Activity in the Prefrontal Cortex during Motor Imagery of Precision Gait: An fNIRS Study," Experimental Brain Research, vol. 238, no. 1, pp. 221–228, 2020.

[23] L. Almulla, I. Al-Naib, I. S. Ateeq and M. Althobaiti, "Observation and Motor Imagery Balance Tasks Evaluation: An fNIRS Feasibility Study," PLoS One, vol. 17, no. 3, p. e0265898, Mar. 2022.

[24] S. Glover, E. Bibby and E. Tuomi, "Executive Functions in Motor Imagery: Support for the Motor-cognitive Model over the Functional Equivalence Model," Experimental Brain Research, vol. 238, no. 4, pp. 931–944, DOI: 10.1007/s00221-020-05756-4, Apr. 2020.

[25] J. A. Wilson, G. Schalk, L. M. Walton and J. C. Williams, "Using an EEG-based Brain-Computer Interface for Virtual Cursor Movement with BCI2000," Journal of Visualized Experiments, no. 29, DOI: 10.3791/1319, Jul. 2009.

[26] S. S. Moumgiakmas and G. A. Papakostas, "Robustly Effective Approaches on Motor Imagery-based Brain Computer Interfaces," Computers, vol. 11, no. 5, p. 61, DOI: 10.3390/computers11050061, 2022.

[27] S. Selim, M. Tantawi, H. Shedeed and A. Badr, "A Comparative Analysis of Different Feature Extraction Techniques for Motor Imagery Based BCI System," Proc. of the Int. Conf. on Artificial Intelligence and Computer Vision (AICV2020), pp. 740–749, DOI: 10.1007/978-3-030-44289-7_69, 2020.

[28] J. Camacho and V. Manian, "Real-time Single Channel EEG Motor Imagery Based Brain Computer Interface," Proc. of the IEEE 2016 World Automation Congress (WAC), pp. 1–6, DOI: 10.1109/WAC.2016.7582973, Rio Grande, PR, USA, Jul. 2016.

[29] L.-W. Ko, S. S. K. Ranga, O. Komarov and C.-C. Chen, "Development of Single-channel Hybrid BCI System Using Motor Imagery and SSVEP," J. of Healthcare Eng., vol. 2017, pp. 1–7, DOI: 10.1155/2017/3789386, 2017.

[30] R. Chen et al., "Enhancement of Time-frequency Energy for the Classification of Motor Imagery Electroencephalogram Based on an Improved FitzHugh–Nagumo Neuron System," IEEE Transactions on Neural Systems and Rehabilitation Engineering, vol. 31, pp. 282–293, 2023.

[31] G. Rodríguez-Bermúdez and P. J. García-Laencina, "Automatic and Adaptive Classification of Electroencephalographic Signals for Brain Computer Interfaces," J. of Medical Systems, vol. 36, no. S1, pp. 51–63, DOI: 10.1007/s10916-012-9893-4, Nov. 2012.

[32] R. R. Sharma and R. B. Pachori, "A New Method for Non-stationary Signal Analysis Using Eigenvalue Decomposition of the Hankel Matrix and Hilbert Transform," Proc. of the 2017 4th IEEE Int. Conf. on Signal Processing and Integrated Networks (SPIN), pp. 484–488, DOI: 10.1109/SPIN.2017.8049998, Feb. 2017.

[33] J. Kevric and A. Subasi, "Comparison of Signal Decomposition Methods in Classification of EEG Signals for Motor-imagery BCI System," Biomed. Signal Process. Control, vol. 31, pp. 398–406, DOI: 10.1016/j.bspc.2016.09.007, Jan. 2017.

[34] O. Attallah, J. Abougharbia, M. Tamazin and A. A. Nasser, "A BCI System Based on Motor Imagery for Assisting People with Motor Deficiencies in the Limbs," Brain Sciences, vol. 10, no. 11, p. 864, DOI: 10.3390/brainsci10110864, Nov. 2020.

[35] Ji, Ma, Dong and Zhang, "EEG Signals Feature Extraction Based on DWT and EMD Combined with Approximate Entropy," Brain Sciences, vol. 9, no. 8, p. 201, DOI: 10.3390/brainsci9080201, Aug. 2019.

[36] A. al-Qerem, F. Kharbat, S. Nashwan, S. Ashraf and K. Blaou, "General Model for Best Feature Extraction of EEG Using Discrete Wavelet Transform Wavelet Family and Differential Evolution," Int. J. of Distributed Sensor Networks, vol. 16, no. 3, p. 155014772091100, Mar. 2020.

[37] G. C. Jana, A. Agrawal, P. K. Pattnaik and M. Sain, "DWT-EMD Feature Level Fusion Based Approach over Multi and Single Channel EEG Signals for Seizure Detection," Diagnostics, vol. 12, no. 2, p. 324, DOI: 10.3390/diagnostics12020324, Jan. 2022.

[38] B. Blankertz et al., "The BCI Competition III: Validating Alternative Approaches to Actual BCI Problems," IEEE Transactions on Neural Systems and Rehabilitation Engineering, vol. 14, no. 2, pp. 153–159, DOI: 10.1109/TNSRE.2006.875642, Jun. 2006.

[39] M.-H. Lee et al., "EEG Dataset and OpenBMI Toolbox for Three BCI Paradigms: An Investigation into BCI Illiteracy," Gigascience, vol. 8, no. 5, DOI: 10.1093/gigascience/giz002, May 2019.

[40] S. Kanoga, A. Kanemura and H. Asoh, "A Comparative Study of Features and Classifiers in Single-channel EEG-based Motor Imagery BCI," Proc. of the 2018 IEEE Global Conf. on Signal and Information Processing (GlobalSIP), pp. 474–478, DOI: 10.1109/GlobalSIP.2018.8646636, Nov. 2018.

[41] M. Al-Quraishi, I. Elamvazuthi, S. Daud, S. Parasuraman and A. Borboni, "EEG-based Control for Upper and Lower Limb Exoskeletons and Prostheses: A Systematic Review," Sensors, vol. 18, no. 10, p. 3342, DOI: 10.3390/s18103342, Oct. 2018.

[42] H. U. Amin et al., "Feature Extraction and Classification for EEG Signals Using Wavelet Transform and Machine Learning Techniques," Australasian Physical and Engineering Sciences in Medicine, vol. 38, no. 1, pp. 139–149, DOI: 10.1007/s13246-015-0333-x, Mar. 2015.

[43] A. A. Abdul-latif, I. Cosic, D. K. Kumar, B. Polus and C. da_Costa, "Power Changes of EEG Signals Associated with Muscle Fatigue: The Root Mean Square Analysis of EEG Bands," Proc. of the 2004 Intelligent Sensors, Sensor Networks and Information Processing Conf., pp. 531–534, DOI: 10.1109/ISSNIP.2004.1417517, 2004.

[44] B. Hjorth, "EEG Analysis Based on Time Domain Properties," Electroencephalography and Clinical Neurophysiology, vol. 29, no. 3, pp. 306–310, DOI: 10.1016/0013-4694(70)90143-4, Sep. 1970.

[45] M. S. Safi and S. M. M. Safi, "Early Detection of Alzheimer's Disease from EEG Signals Using Hjorth Parameters," Biomed. Signal Process. Control, vol. 65, p. 102338, DOI: 10.1016/j.bspc.2020.102338, 2021.

[46] F. Lotte, "A New Feature and Associated Optimal Spatial Filter for EEG Signal Classification: Waveform Length," Proc. of the 21st Int. Conf. on Pattern Recognition (ICPR2012), pp. 1302–1305, Tsukuba, Japan, 2012.

[47] D. Garrett, D. A. Peterson, C. W. Anderson and M. H. Thaut, "Comparison of Linear, Nonlinear and Feature Selection Methods for EEG Signal Classification," IEEE Transactions on Neural Systems and Rehabilitation Engineering, vol. 11, no. 2, pp. 141–144, DOI: 10.1109/TNSRE.2003.814441, Jun. 2003.

[48] P. Nadkarni, "Core Technologies: Machine Learning and Natural Language Processing," Clinical Research Computing, pp. 85–114, DOI: 10.1016/B978-0-12-803130-8.00004-X, Elsevier, 2016.

[49] S. Dreiseitl and L. Ohno-Machado, "Logistic Regression and Artificial Neural Network Classification Models: A Methodology Review," J. of Biomedical Informatics, vol. 35, no. 5–6, pp. 352–359, Oct. 2002.

[50] Y. Huang and L. Li, "Naive Bayes Classification Algorithm Based on Small Sample Set," Proc. of the 2011 IEEE Int. Conf. on Cloud Computing and Intelligence Systems, pp. 34–39, DOI: 10.1109/CCIS.2011.6045027, Sep. 2011.

[51] Pawan and R. Dhiman, "Motor Imagery Signal Classification Using Wavelet Packet Decomposition and Modified Binary Grey Wolf Optimization," Measurement: Sensors, vol. 24, p. 100553, DOI: 10.1016/j.measen.2022.100553, Dec. 2022.

[52] M. Ahn, H. Cho, S. Ahn and S. C. Jun, "High Theta and Low Alpha Powers May Be Indicative of BCI-illiteracy in Motor Imagery," PLoS One, vol. 8, no. 11, p. e80886, Nov. 2013.

[53] G. Roy, A. K. Bhoi and S. Bhaumik, "A Comparative Approach for MI-Based EEG Signals Classification Using Energy, Power and Entropy," IRBM, vol. 43, no. 5, pp. 434–446, Oct. 2022.

ملخص البحث:

لقد ثبت نجاح استخدام بينيّةٍ تربط الدّماغ بالحاسوب مبنيّة على التّصوير الحركي كآلية تحكّم مع قنوات متعدّدة لتصوير الدّماغ. ولأغراضٍ عمليةٍ، فإنّ من المفضّل تقليل عدد قنوات صور تخطيط الدّماغ.

هذه الورقة تبحث في قناةٍ مفردةٍ لصور تخطيط الدّماغ في سياق التّصوير الحركي. علاوة على ذلك، فإنّ عدد السِّمات الّتي يمكن استخلاصها من نظامٍ ذي قناةٍ واحدة يكون غير كافٍ، لذا فإنّ استخدام تقنيةٍ فعّالةٍ لاستخلاص السِّمات يلعب دوراً حاسماً في التّغلُّب على هذا المحدِّد.

من هنا، تقترح هذه الورقة دمج استخلاص السِّمات بواسطة الانتقال المجرَّد للمويجات وبواسطة المجال الزّمني من أجل توفير معلوماتٍ أدقّ لأغراض التّصنيف. وقد تمّ تجريب التّقنية المقترحة على مجموعتي بياناتٍ؛ إذ تمّ الحصول على دقّةٍ وصلت إلى 87.5% باستخدام الانحدار اللّوجستي، بينما بلغت الدّقّة 93% باستخدام آلة متّجهات الدّعم (SVM) للتّصنيف. وعند تناول احتمالية تحسين الأداء لقناةٍ مفردة توضع على جبهة الشّخص المفحوص، وكانت النتائج واعِدة.